atoms

MDPI

Article

Experimental Cross Sections for Electron-Impact Single, Double, and Triple Ionization of La^+

B. Michel Döhring [1,2,*], Alexander Borovik, Jr. [1], Florian Gocht [1], Kurt Huber [1] and Stefan Schippers [1,2]

[1] I. Physikalisches Institut, Justus-Liebig-Universität Gießen, 35392 Giessen, Germany
[2] Helmholtz Forschungsakademie Hessen für FAIR (HFHF), GSI Gesellschaft für Schwerionenforschung, Campus Gießen, 35392 Giessen, Germany
* Correspondence: michel.doehring@exp1.physik.uni-giessen.de

Abstract: We report on new measurements of absolute cross sections for single, double, and triple electron-impact ionization of singly charged lanthanum ions. The resulting single and double ionization cross sections are in fair agreement with results from previous experimental work. In the present work, we extended the experimental range by a factor of two to approx. 2000 eV. To the best of our knowledge, there have been no previous measurements of triple ionization. The present work in progress aims to provide vitally needed atomic data for the astrophysical modeling of kilonovae.

Keywords: electron-impact ionization of ions; crossed-beams experiment; lanthanum ions; kilonovae

1. Introduction

In 2017, the LIGO/Virgo collaboration detected the first gravitational-wave signal from the merger of a neutron-star binary [1]. Less than two seconds later, a short gamma-ray burst was detected, followed by a several-days-lasting optical "afterglow" powered by the radioactive decay of the neutron-rich material ejected in the merger, i.e., a kilonova [2]. This first optical observation of the aftermath of a neutron-star merger has triggered synergetic research activities, with atomic physics being heavily involved. Kilonova light-curves and spectra reveal the abundances of the heavy chemical elements (lanthanides, actinides) that are produced in the preceding violent neutron-star merger events [3–5]. In order to be able to reliably conclude elemental abundances from the astronomical observations, atomic data are required for the basic atomic processes that occur in the afterglow. The rapidly growing number of theory papers on the atomic properties of heavy elements (e.g., [6–14]) testifies to the current interest.

So far, local thermodynamic equilibrium (LTE) conditions have mostly been assumed in the astrophysical modeling of kilonovae [3,4,15,16], which is certainly an oversimplification, given the highly dynamic and transient nature of the phenomenon. Only very recently, the impact of non-LTE effects on kilonovae has been estimated [17,18], highlighting the need for accurate atomic cross sections and rate coefficients. Generally, such quantities cannot be easily calculated, if at all, with a sufficient precision for the heavy many-electron ions of interest. The currently available atomic data for heavy elements mostly stem from theoretical calculations with limited accuracy. This affects basic atomic quantities such as energy levels and transition rates (see, e.g., [19]) and, therefore, the cross sections of atomic collision processes.

Electron-impact ionization (EII) is an important atomic collision process, which decisively determines the charge balance in collisionally ionized plasmas. For heavy elements,

check for updates

Academic Editors: John Sheil and Jean-Christophe Pain

Received: 28 December 2024
Revised: 20 January 2025
Accepted: 26 January 2025
Published: 28 January 2025

Citation: Döhring, B.M.; Borovik, A., Jr.; Gocht, F.; Huber, K.; Schippers, S. Experimental Cross Sections for Electron-Impact Single, Double, and Triple Ionization of La^+. *Atoms* **2025**, *13*, 14. https://doi.org/10.3390/atoms13020014

the number of experimental EII studies is quite limited. Table 1 provides a comprehensive overview of experimental cross sections for the EII of elements with nuclear charges $Z \geq 55$, i.e., for elements heavier than xenon. In all these studies, the experimental collision energy was limited to maximally 1000 eV.

Table 1. List of experimental cross sections for electron-impact ionization of positively charged atomic ions heavier than xenon that are available from the literature.

Element	Nuclear Charge	Ion Charge	Energy Range (eV)	Reference
Cs	55	1	20–100	[20]
Cs	55	1	25–5000	[21]
Cs	55	1	50–130	[22]
Ba	56	1	9–30	[23]
Ba	56	2–3	10–1000	[24]
Ba	56	1–13	700–900	[25]
La	57	1–3	10–1000	[26]
Sm	62	1–12	10–1000	[27]
Hf	72	3	30–1000	[28]
Ta	73	3	25–300	[28]
W	74	1–10	10–1000	[29]
W	74	11–19	100–1000	[30]
Pb	82	1–10	10–1000	[31]
Bi	83	1–10	10–1000	[32]

In order to meet the demands for astrophysical data, we set out to provide experimental cross sections for electron-impact ionization of lanthanum and lanthanide ions. The present pilot study included single, double, and triple ionization of La^+ ions over an extended range of collision energies up to about 2000 eV using a recently commissioned high-intensity electron gun [33]. For energies up to 1000 eV, the single and double ionization cross sections were compared with the earlier results of Müller et al. [26]. To the best of our knowledge, there have been no previous experimental results for electron-impact triple ionization of La^+ ions.

2. Experiment

The measurements were carried out at the Giessen electron–ion crossed-beams setup, which has been routinely used for the measurement of absolute EII cross sections for many years [30,34,35]. General descriptions of the experimental and data-analysis procedures can be found, e.g., in [34,36]. In the present experiment, solid lanthanum was evaporated in an electrically heated oven, which was placed in the plasma chamber of an all-permanent-magnet 10-GHz ECR ion source [37]. The heating power was in the range 50–75 W. In addition to the lanthanum vapor, helium was leaked into the ion source, in order to ensure stable plasma conditions. The source was operated at an electric potential of 12 kV. This allowed for efficient extraction of the ion beam towards the electrically grounded ion beam line. A first dipole electromagnet was used for the selection of the desired $^{139}La^+$ ions according to their mass/charge ratio (Figure 1). Shortly before entering the electron–ion scattering chamber, the ion beam was bent with a 90° electrostatic deflector and collimated by two sets of four-jaw slits, which were adjusted to openings with diameters between 0.1 and 1.6 mm, depending on the measurement mode (see below). The collimated ion current amounted up to several hundred pA. In the scattering chamber, the collimated ion beam was crossed by a ribbon-shaped electron beam [33] under an angle of 90° in the laboratory frame.

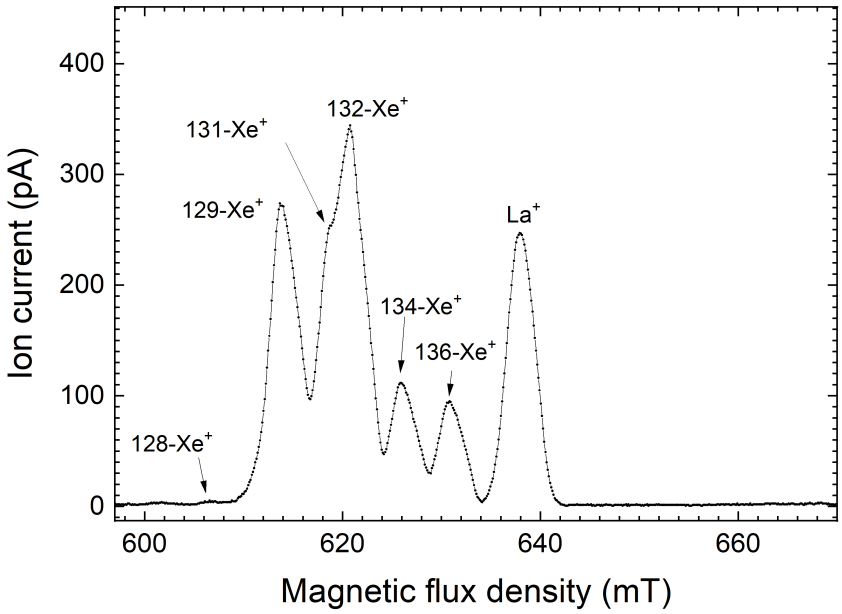

Figure 1. Measured mass/charge spectrum obtained by scanning the first dipole magnet. For unambiguous identification of La^+, a small admixture of xenon was used, which can be easily identified by its natural abundance pattern. Note that isotopic resolution could have been achieved by further ion-beam collimation before and behind the analyzing magnet.

The La^{2+}, La^{3+}, and La^{4+} product ions resulting from single, double, and triple ionization of La^+, respectively, were separated from the primary La^+ ion by a second dipole electromagnet and directed onto a single particle detector [38]. The primary ions were collected in a Faraday cup. Since separate magnet settings were required for each product-ion charge state, the present single, double, and triple ionization measurements had to be carried out consecutively. Absolute cross sections were obtained by normalizing the measured product-ion count rates on the constantly monitored electron and ion currents and on the geometrical beam overlap. The latter was determined by employing the animated-beams technique [39], as implemented by Müller et al. [36]. In order to ensure a 100% collection efficiency of primary and product ions, the ion beam was tightly collimated to a diameter of 1.0 mm in the horizontal and vertical directions.

In addition to these *absolute* cross section measurements, which were carried out for a limited set of electron energies, we also performed *scan* measurements, where the electron energy was swiftly changed over a millisecond timescale in small energy steps to average out the influence of beam-overlap variations on the measured count rates. This was particularly useful for uncovering resonance contributions to the measured EII cross sections (see, e.g., [40–43]). The scanning required fast control of virtually all the electron gun's high-voltage supplies. The associated electronics hardware and software were newly developed for the present electron gun and will be described in detail elsewhere [44]. For the scan measurements, the electron gun was positioned such that the beam overlap was at its maximum and the ion beam diameter was enlarged to 1.6 mm in each direction. In the data analysis, the relative scan cross sections were finally scaled to the separately measured absolute cross sections.

3. Results

Figure 2 presents our experimental cross sections for electron-impact single ionization of La^+, together with the previous results of Müller et al. [26]. At energies below approx. 200 eV, our cross sections were larger than the earlier ones. We attribute this to the different fractions of metastable ions in the respective primary beams. The differences in metastable

fractions are related to the conditions of the different ion sources used. Müller et al. used a sputter Penning ion source. In principle, the presence of metastable ions is revealed by nonzero ionization cross sections below the single-ionization threshold of La^+([Xe] $5d^2\ ^3F_2$) ground-level ions at 11.185 eV [45]. Because this energy is almost below the operational limit of our electron gun, we were not able to measure at a sufficient number of below-threshold energies to make a more definitive statement. At energies above 200 eV, both sets of cross sections converge. Our new data extend the energy range by a factor of two, i.e., from 1000 eV previously to 2000 eV presently. The relatively large error bars for the present absolute measurements stem from the comparatively low and unstable ion currents that were delivered by the ECR ion source.

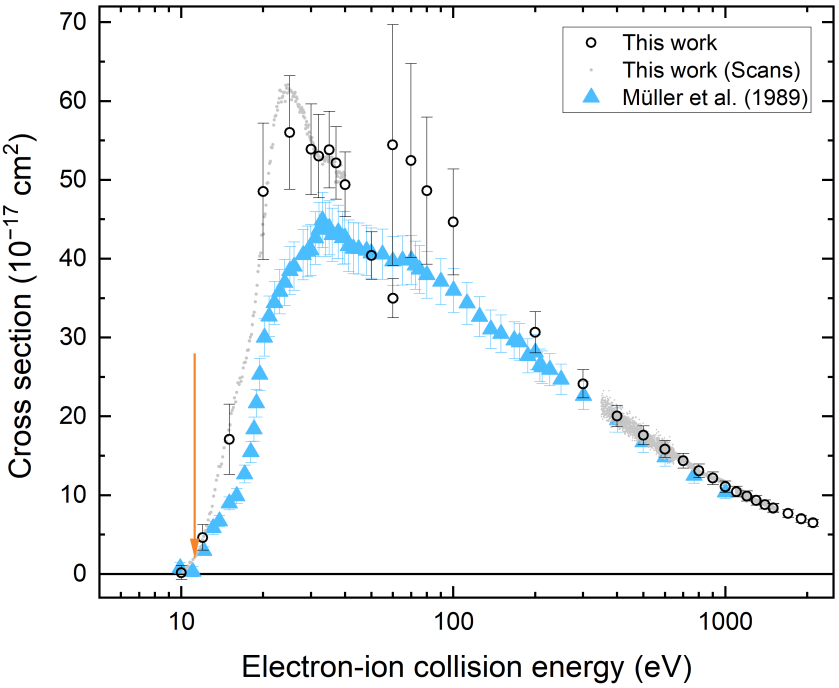

Figure 2. Experimental cross sections of electron-impact *single* ionization of La^+. The large open symbols represent our present absolute cross sections. The error bars comprise systematic and two-sigma statistical uncertainties. The small grey symbols resulted from the present scan measurements. The corresponding error bars represent the two-sigma statistical uncertainties. The full triangles are the data of Müller et al. [26]. The vertical arrow at 11.185 eV [45] marks the threshold for single ionization of ground-level La^+.

The present and previously published [26] cross sections for electron-impact double ionization of La^+ are shown in Figure 3. In the 10–60 eV energy range, the electron gun was operated in a 'high-current' mode, where the electron current increased steeply with increasing electron energy. At energies above 60 eV, the electron current had to be limited to prevent overheating and the 'high-energy' mode [33] was used, where the increase in the electron current with increasing electron energy is much less pronounced than in the 'high-current' mode. It is reassuring that the resulting cross sections are independent of the operation mode within the experimental error bars, as should be the case.

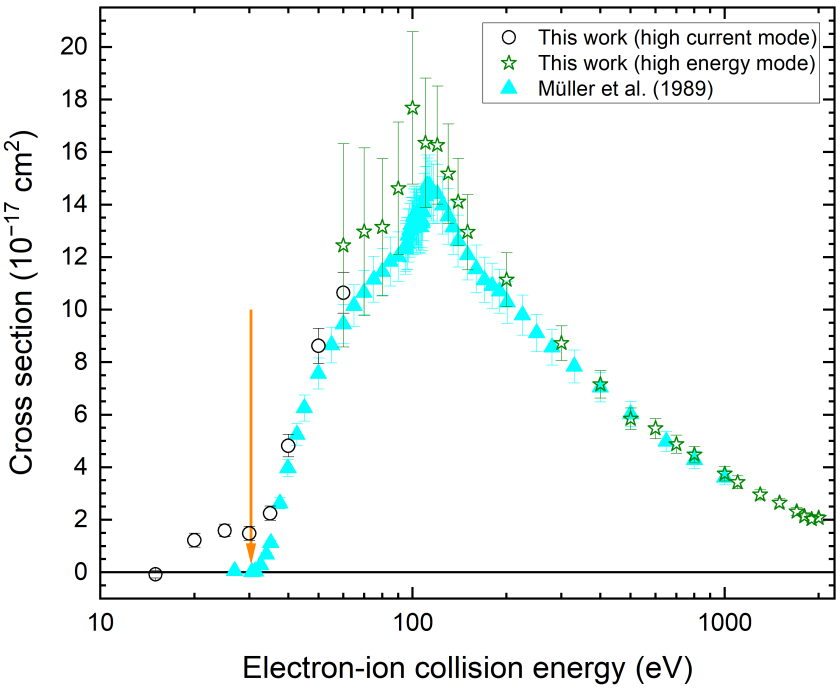

Figure 3. Experimental cross sections of electron-impact *double* ionization of La^+. The open circles and stars represent our presents absolute cross sections. The different types of symbols represent different operation modes of the electron gun. The error bars comprise systematic and two-sigma statistical uncertainties. The full triangles are the data of Müller et al. [26]. The vertical arrow at 30.362 eV marks the threshold for double ionization of ground-level La^+.

The agreement between the present and the previous data is better than for single ionization. This indicates that the cross sections for double ionization of ground-state and metastable ions are of about equal magnitude. The presence of metastable ions in the present experiment is obvious from the fact that there was a significantly nonzero cross section extending to at least 10 eV below the threshold for double ionization at 30.362 eV. According to the NIST Atomic Spectra Database [45], fine-structure levels of the even-parity [Xe] $4f^2$ configuration have excitation energies of up to 8.6 eV. We can only speculate that these levels are sufficiently long-lived such that they survive the transport from the ion source to the electron–ion interaction region and, thus, contribute to the measured cross section below the ground-level ionization threshold.

Figure 4 displays our experimental cross section for electron-impact triple ionization of La^+. To our knowledge this has not been measured before. The threshold for ground-level ionization was at 80.31 eV [45], i.e., below our experimental energy range.

The magnitude of the cross sections decreased with increasing product-ion charge state. The maximum of the double-ionization cross section was approximately a factor of three lower than the maximum of the single-ionization cross section. The maximum of the triple-ionization cross section was another factor of ten lower. Figure 5 shows the ratios of our measured cross sections over the entire experimental energy range. In view of the work of Hahn et al. [46], who pointed out the significance of electron-impact multiple ionization for the calculation of the charge balances of lighter elements, even the triple ionization cross section should be important for an accurate modeling of kilonovae.

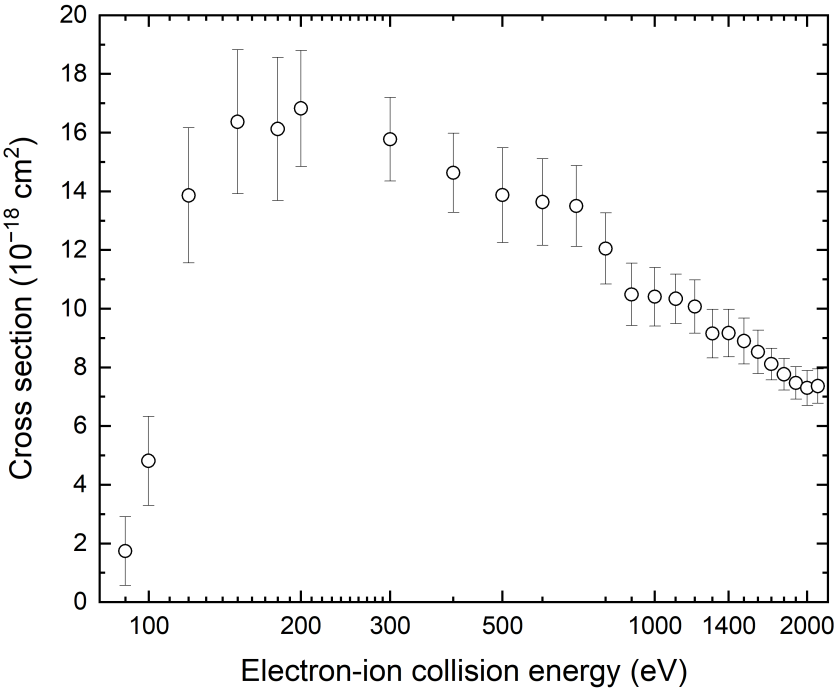

Figure 4. Experimental cross sections for electron-impact *triple* ionization of La^+. The error bars comprise systematic and two-sigma statistical uncertainties. The threshold for triple ionization of ground-level La^+ was at 80.31 eV [45].

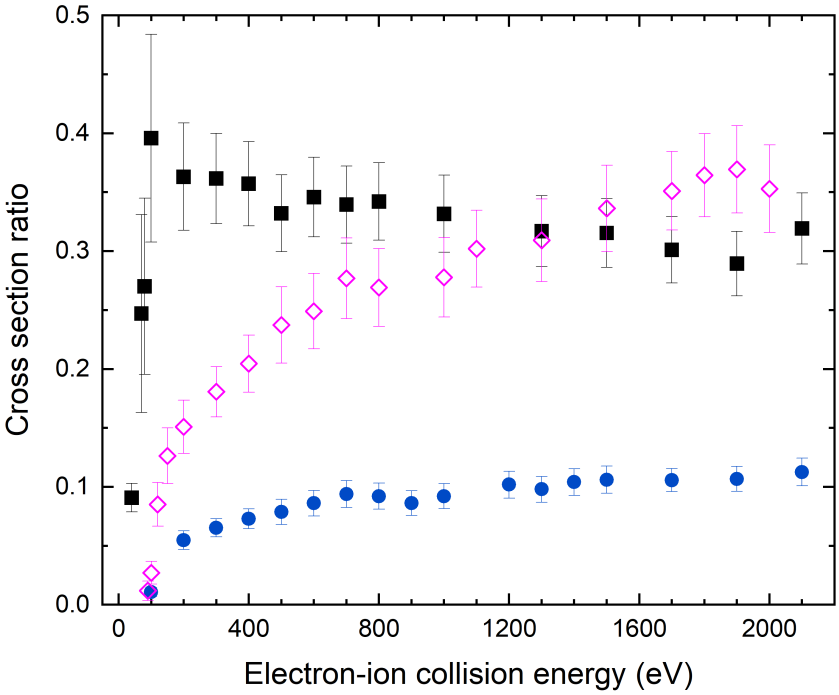

Figure 5. Experimental cross section ratios: double/single ionization (black full squares), triple/single ionization (blue full circles), and triple/double ionization (magenta open diamonds).

4. Summary and Outlook

We presented the first results from work in progress on electron-impact single and multiple ionization of lanthanum and lanthanide ions, aiming to provide experimental cross sections for kilonova modeling. For single and double ionization of La^+, our measured cross sections agree with the existing data from the literature, except at low energies where the presence of metastable primary ions affected the experimental cross sections,

in particular, for single ionization. As compared to earlier works, we have considerably extended the experimental energy range by a factor of two. In addition, we measured the cross section for triple ionization, which was one order of magnitude smaller than the single ionization cross section. Nevertheless, this should still be relevant for the modeling of the lanthanum charge balance in a collisionally ionized plasma.

In the past two years, we have moved our electron–ion crossed-beams setup to a new location, where we will couple it with a more powerful ECR ion source. In the future, part of our research will be devoted to providing even more accurate and vitally needed cross sections for electron-impact ionization of lanthanide ions. We also hope to inspire corresponding future theoretical work.

Author Contributions: Conceptualization, B.M.D. and S.S.; methodology, B.M.D., A.B.J. and K.H.; software, K.H.; investigation, B.M.D., A.B.J. and F.G.; formal analysis, B.M.D. and F.G., writing—original draft preparation, B.M.D. and S.S.; funding acquisition: S.S. All authors have read and agreed to the published version of the manuscript.

Funding: Financial support was provided by the German Federal Ministry for Education and Research (Bundesministerium für Bildung und Forschung, BMBF) via the Collaborative Research Center ErUM-FSP T05—"Aufbau von APPA bei FAIR" (Grant Nos. 05P21RGFA1 and 05P24RG2) and by the State of Hesse via the Research Cluster ELEMENTS (Project ID 500/10.006).

Data Availability Statement: The data are available from the authors upon reasonable request.

Conflicts of Interest: The authors declare no conflicts of interest.

References

1. Abbott, B.P.; Abbott, R.; Abbott, T.D.; Acernese, F.; Ackley, K.; Adams, C.; Adams, T.; Addesso, P.; Adhikari, R.X.; Adya, V.B.; et al. GW170817: Observation of Gravitational Waves from a Binary Neutron Star Inspiral. *Phys. Rev. Lett.* **2017**, *119*, 161101. [CrossRef] [PubMed]
2. Metzger, B.D. Kilonovae. *Living Rev. Relativ.* **2020**, *23*, 1. [CrossRef]
3. Kasen, D.; Metzger, B.; Barnes, J.; Quataert, E.; Ramirez-Ruiz, E. Origin of the heavy elements in binary neutron-star mergers from a gravitational-wave event. *Nature* **2017**, *551*, 80–84. [CrossRef] [PubMed]
4. Watson, D.; Hansen, C.J.; Selsing, J.; Koch, A.; Malesani, D.B.; Andersen, A.C.; Fynbo, J.P.U.; Arcones, A.; Bauswein, A.; Covino, S.; et al. Identification of strontium in the merger of two neutron stars. *Nature* **2019**, *574*, 497. [CrossRef] [PubMed]
5. Holmbeck, E.M.; Barnes, J.; Lund, K.A.; Sprouse, T.M.; McLaughlin, G.C.; Mumpower, M.R. Superheavy elements in kilonovae. *Astrophys. J.* **2023**, *951*, L13. [CrossRef]
6. Radžiūtė, L.; Gaigalas, G.; Kato, D.; Rynkun, P.; Tanaka, M. Extended Calculations of Energy Levels and Transition Rates for Singly Ionized Lanthanide Elements. I. Pr–Gd. *Astrophys. J.* **2020**, *248*, 17. [CrossRef]
7. Domoto, N.; Tanaka, M.; Wanajo, S.; Kawaguchi, K. Signatures of r-process elements in kilonova spectra. *Astrophys. J.* **2021**, *913*, 26. [CrossRef]
8. Carvajal Gallego, H.; Berengut, J.C.; Palmeri, P.; Quinet, P. Atomic data and opacity calculations in La V–X ions for the investigation of kilonova emission spectra. *Mon. Not. R. Astron. Soc.* **2022**, *513*, 2302. [CrossRef]
9. Banerjee, S.; Tanaka, M.; Kato, D.; Gaigalas, G.; Kawaguchi, K.; Domoto, N. Opacity of the highly ionized lanthanides and the effect on the early kilonova. *Astrophys. J.* **2022**, *934*, 117. [CrossRef]
10. Domoto, N.; Tanaka, M.; Kato, D.; Kawaguchi, K.; Hotokezaka, K.; Wanajo, S. Lanthanide features in near-infrared spectra of kilonovae. *Astrophys. J.* **2022**, *939*, 8. [CrossRef]
11. Ben Nasr, S.; Carvajal Gallego, H.; Deprince, J.; Palmeri, P.; Quinet, P. Atomic data and expansion opacity calculations in two representative 4d transition elements, niobium and silver, of interest for kilonovae studies. *Astron. Astrophys.* **2023**, *678*, A67. [CrossRef]
12. Bondarev, A.I.; Gillanders, J.H.; Cheung, C.; Safronova, M.S.; Fritzsche, S. Calculations of multipole transitions in Sn II for kilonova analysis. *Eur. Phys. J. D* **2023**, *77*, 126. [CrossRef]
13. Ben Nasr, S.; Carvajal Gallego, H.; Deprince, J.; Palmeri, P.; Quinet, P. Comparative study of kilonova opacities for three elements of the sixth period (hafnium, osmium, and gold) from new atomic structure calculations in Hf I-IV, Os I-IV, and Au I-IV. *Astron. Astrophys.* **2024**, *687*, A41. [CrossRef]

14. Gaigalas, G.; Rynkun, P.; Domoto, N.; Tanaka, M.; Kato, D.; Kitovienė, L. Theoretical investigation of energy levels and transitions for Ce III with applications to kilonova spectra. *Mon. Not. R. Astron. Soc.* **2024**, *530*, 5220. [CrossRef]
15. Metzger, B.D.; Martínez-Pinedo, G.; Darbha, S.; Quataert, E.; Arcones, A.; Kasen, D.; Thomas, R.; Nugent, P.; Panov, I.V.; Zinner, N.T. Electromagnetic counterparts of compact object mergers powered by the radioactive decay of r-process nuclei. *Mon. Not. R. Astron. Soc.* **2010**, *406*, 2650–2662. [CrossRef]
16. Tanaka, M.; Hotokezaka, K. Radiative transfer simulations of neutron star merger ejecta. *Astrophys. J.* **2013**, *775*, 113. [CrossRef]
17. Hotokezaka, K.; Tanaka, M.; Kato, D.; Gaigalas, G. Nebular emission from lanthanide-rich ejecta of neutron star merger. *Mon. Not. R. Astron. Soc.* **2021**, *506*, 5863. [CrossRef]
18. Pognan, Q.; Grumer, J.; Jerkstrand, A.; Wanajo, S. NLTE spectra of kilonovae. *Mon. Not. R. Astron. Soc.* **2023**, *526*, 5220. [CrossRef]
19. Quinet, P.; Palmeri, P. Current status and developments of the atomic database on rare-earths at Mons University (DREAM). *Atoms* **2020**, *8*, 18. [CrossRef]
20. Peart, B.; Dolder, K. Measurements of cross sections for inner- and outer-shell ionization of Rb^+, Cs^+, Ca^+ and Sr^+ ions by electron impact. *J. Phys. B* **1975**, *8*, 56. [CrossRef]
21. Hertling, D.R.; Feeney, R.K.; Hughes, D.W.; Sayle II, W.E. Absolute experimental cross sections for the electron impact single, double, triple, and quadruple ionization of Cs+ ions. *J. Appl. Phys.* **1982**, *53*, 5427. [CrossRef]
22. Thomason, J.W.G.; Peart, B.; Hayton, S.J.T. The double ionization of Cs^+ and Sr^+ by energy-resolved electrons. *J. Phys. B* **1997**, *30*, 749–756. [CrossRef]
23. Peart, B.; Underwood, J.R.A.; Dolder, K. Autoionisation and threshold ionisation of Ba^+ by energy-resolved electrons. *J. Phys. B* **1989**, *22*, 1679. [CrossRef]
24. Tinschert, K.; Müller, A.; Hofmann, G.; Salzborn, E. Electron-impact single and double ionization of Ba^{2+} and Ba^{3+} ions. *Phys. Rev. A* **1991**, *43*, 3522–3534. [CrossRef] [PubMed]
25. Knopp, H.; Böhme, C.; Jacobi, J.; Ricz, S.; Schippers, S.; Müller, A. Electron-impact multiple ionization of Ba^{q+} ions ($1 \leq q \leq 13$) via resonant 3d excitation. *Nucl. Instrum. Methods Phys. Res. B* **2003**, *205*, 433. [CrossRef]
26. Müller, A.; Tinschert, K.; Hofmann, G.; Salzborn, E.; Dunn, G.H.; Younger, S.M.; Pindzola, M.S. Electron-impact ionization of La^{q+} ions ($q = 1, 2, 3$). *Phys. Rev. A* **1989**, *40*, 3584–3598. [CrossRef] [PubMed]
27. Aichele, K.; Arnold, W.; Hathiramani, D.; Scheuermann, F.; Salzborn, E.; Mitnik, D.M.; Griffin, D.C.; Colgan, J.; Pindzola, M.S. Experimental and theoretical study of electron-impact ionization of atomic ions in the Sm isonuclear sequence. *Phys. Rev. A* **2001**, *64*, 052706. [CrossRef]
28. Falk, R.A.; Dunn, G.H.; Gregory, D.C.; Crandall, D.H. Measurement of the contribution of excitation autoionization to electron-impact ionization of ions: Ti^{3+}, Zr^{3+}, Hf^{3+}, and Ta^{3+}. *Phys. Rev. A* **1983**, *27*, 762–770. [CrossRef]
29. Stenke, M.; Aichele, K.; Harthiramani, D.; Hofmann, G.; Steidl, M.; Völpel, R.; Salzborn, E. Electron-impact single-ionization of singly and multiply charged tungsten ions. *J. Phys. B* **1995**, *28*, 2711–2721. [CrossRef]
30. Schury, D.; Borovik Jr., A.; Ebinger, B.; Spruck, K.; Jin, F.; Müller, A.; Schippers, S. Electron-impact single ionisation of W^{q+} ions: Experiment and theory for $11 \leq q \leq 18$. *J. Phys. B* **2020**, *53*, 015201. [CrossRef]
31. Loch, S.D.; Ludlow, J.A.; Pindzola, M.S.; Scheuermann, F.; Kramer, K.; Fabian, B.; Huber, K.; Salzborn, E. Electron-impact ionization of Pb^{q+} ions for $q = 1 - 10$. *Phys. Rev. A* **2005**, *72*, 032713. [CrossRef]
32. Loch, S.D.; Pindzola, M.S.; Badnell, N.R.; Scheuermann, F.; Kramer, K.; Huber, K.; Salzborn, E. Electron-impact ionization of Bi^{q+} for $q = 1 - 10$. *Phys. Rev. A* **2004**, *70*, 052714. [CrossRef]
33. Ebinger, B.; Borovik, A., Jr.; Molkentin, T.; Müller, A.; Schippers, S. Commissioning of a powerful electron gun for electron-ion crossed-beams experiments. *Nucl. Instrum. Methods Phys. Res. B* **2017**, *408*, 317. [CrossRef]
34. Jacobi, J.; Knopp, H.; Schippers, S.; Müller, A.; Loch, S.D.; Witthoeft, M.; Pindzola, M.S.; Ballance, C.P. Strong contributions of indirect processes to the electron-impact ionization cross section of Sc^+ ions. *Phys. Rev. A* **2004**, *70*, 042717. [CrossRef]
35. Jin, F.; Borovik, A.; Döhring, B.M.; Ebinger, B.; Müller, A.; Schippers, S. Experimental and theoretical total cross sections for single and double ionization of the open-4d-shell ions Xe^{12+}, Xe^{13+}, and Xe^{14+} by electron impact. *Eur. Phys. J. D* **2024**, *78*, 68. [CrossRef]
36. Müller, A.; Huber, K.; Tinschert, K.; Becker, R.; Salzborn, E. An improved crossed-beams technique for the measurement of absolute cross sections for electron impact ionisation of ions and its application to Ar^+ ions. *J. Phys. B* **1985**, *18*, 2993. [CrossRef]
37. Brötz, F.; Trassl, R.; McCullough, R.W.; Arnold, W.; Salzborn, E. Design of compact all-permanent magnet electron cyclotron resonance (ECR) ion sources for atomic physics experiments. *Phys. Scr.* **2001**, *T92*, 278–280. [CrossRef]
38. Rinn, K.; Müller, A.; Eichenauer, H.; Salzborn, E. Development of single-particle detectors for keV ions. *Rev. Sci. Instrum.* **1982**, *53*, 829–837. [CrossRef]
39. Defrance, P.; Brouillard, F.; Claeys, W.; Wassenhove, G.V. Crossed beam measurement of absolute cross sections: An alternative method and its application to the electron impact ionisation of He^+. *J. Phys. B* **1981**, *14*, 103–110. [CrossRef]
40. Müller, A.; Hofmann, G.; Weissbecker, B.; Stenke, M.; Tinschert, K.; Wagner, M.; Salzborn, E. Correlated two-electron transitions in electron-impact ionization of Li^+ ions. *Phys. Rev. Lett.* **1989**, *63*, 758–761. [CrossRef] [PubMed]

41. Müller, A.; Borovik, A.; Huber, K.; Schippers, S.; Fursa, D.V.; Bray, I. Double-*K*-vacancy states in electron-impact single ionization of metastable two-electron $N^{5+}(1s\,2s\,{}^3S_1)$ ions. *Phys. Rev. A* **2014**, *90*, 010701. [CrossRef]
42. Liu, P.; Zeng, J.; Borovik, A.; Schippers, S.; Müller, A. Electron-impact ionization of Xe^{24+} ions: Theory versus experiment. *Phys. Rev. A* **2015**, *92*, 012701. [CrossRef]
43. Ebinger, B.; Liu, P.; Borovik, A., Jr.; Müller, A.; Zeng, J.; Schippers, S. Resonant and nonresonant indirect electron-impact single ionization of beryllium-like carbon ions via K-shell excitation. *J. Phys. B* **2019**, *52*, 035202. [CrossRef]
44. Döhring, B.M.; Borovik, A., Jr.; Huber, K.; Schippers, S. Commissioning of a fine-step electron energy scan-system for electron-ion-crossed-beams experiments. In preparation.
45. Kramida, A.; Ralchenko, Y.; Reader, J.; NIST ASD Team. *NIST Atomic Spectra Database (Version 5.11.0)*; NIST: Gaithersburg, MD, USA, 2023. [CrossRef]
46. Hahn, M.; Müller, A.; Savin, D.W. Electron-impact multiple-ionization cross sections for atoms and ions of helium through zinc. *Astrophys. J.* **2017**, *850*, 122. [CrossRef]